ELSEVIER

Polymer 44 (2003) 1537–1546

polymer

www.elsevier.com/locate/polymer

# Analysis of the damage zone around the crack tip for two rubber-modified epoxy matrices exhibiting different toughenability

María L. Arias, Patricia M. Frontini*, Roberto J.J. Williams

*Institute of Materials Science and Technology (INTEMA), University of Mar del Plata, National Research Council (CONICET), J.B. Justo 4302, 7600 Mar del Plata, Argentina*

Received 8 July 2002; received in revised form 22 October 2002; accepted 25 October 2002

**Abstract**

One inevitable effect of adding soft rubber particles to a rigid polymer is that its yield stress, $\sigma_Y$, is lowered by the stress concentration effect produced by dispersed particles. This effect may be enhanced if a fraction of the added rubber remains dissolved in the matrix, lowering its glass transition temperature, thus producing an extra decrease in $\sigma_Y$. Both effects lead to an increase in the critical stress intensity factor, $K_{IC}$, originated by crack tip blunting. The toughenability of an epoxy matrix may be defined by its ability to promote deformation mechanisms that can increase $K_{IC}$ beyond the value attained by crack tip blunting. The aim of this manuscript was to analyze the toughenability of two different epoxy systems exhibiting similar relative increases in $K_{IC}$ by rubber addition: (a) diglycidylether of bisphenol A (DGEBA) cured with piperidine; (b) DGEBA cured with a stoichiometric amount of 4,4′-diamine-3,3′-dimethyldicyclohexylmethane (3DCM). Both epoxies were modified with 15 wt% CTBN (carboxyl-terminated butadiene-acrylonitrile copolymer), that phase-separated in the course of polymerization. The damage zone around the surviving crack tip produced by the double-notch four-point-bend (DN-4PB) technique, was analyzed for both rubber-modified epoxies by transmission optical microscopy and transmission electron microscopy. For the DGEBA-piperidine system, dilatation bands (croids) and massive shear yielding in the region close to the crack tip, were observed. For the DGEBA-3DCM system, a region of cavitated particles was observed close to the crack tip without any evidence of shear deformation in the matrix. The higher toughenability of the former system compared to the latter, was associated to the different mechanical behavior observed in uniaxial compression tests of the pure epoxy matrices.


*Keywords:* Rubber-modified epoxies; Toughening mechanisms; Double-notch four-point-bend technique

## 1. Introduction

Thermosets exhibit high values of stiffness and strength together with good heat and solvent resistance, due to their cross-linked nature. One major drawback is their poor resistance to impact and crack initiation. Improvements in their fracture resistance result from the blend with different types of modifiers that generally form a second dispersed phase. The most frequently used modifiers are liquid rubbers that phase-separate in the course of polymerization leading to a dispersion of rubber particles in the thermoset matrix [1].

One inevitable effect of adding soft rubber particles to a rigid polymer is that its yield stress, $\sigma_Y$, is lowered by the stress concentration effect produced by dispersed particles. This effect may be enhanced if a fraction of the added rubber remains dissolved in the matrix, lowering its glass transition temperature, thus producing an extra decrease in $\sigma_Y$. Both effects lead to an increase in the critical stress intensity factor, $K_{IC}$, originated by crack tip blunting. The toughenability of an epoxy matrix may be defined by its ability to promote deformation mechanisms that can increase $K_{IC}$ beyond the expected increase produced by the lower yield stress.

The main toughening mechanism present in rubber-modified epoxies is the cavitation of rubber particles followed by void growth and induced shear yielding of the matrix [2]. Shear bands connecting cavitated rubber particles, called ‘dilatation bands’ or ‘croids’, have been observed [3–6]. In these bands voids are not interconnected and their free surface is formed within the rubber phase.

* Corresponding author.
*E-mail address:* pmfronti@fi.mdp.edu.ar (P.M. Frontini).

0032-3861/03/$ - see front matter © 2002 Elsevier Science Ltd. All rights reserved.
PII: S0032-3861(02)00829-7

They propagate by generating peripheral zones of high elastic strain where the matrix becomes strain softened and yields more easily [6]. The eventual strain hardening prevents the occurrence of fracture at relatively early stages of the deformation.

From the description given above, the toughenability of an epoxy matrix might be related to its capacity to exhibit strain softening and large strains at relatively low stress values. The aim of this manuscript is to analyze this relationship for two epoxy systems exhibiting different toughenability: (a) diglycidylether of bisphenol A (DGEBA) cured with piperidine (a classic system for the study of toughening mechanisms), and (b) DGEBA cured with a stoichiometric amount of 4,4′-diamine-3,3′-dimethyl-dicyclohexylmethane (3DCM) (an epoxy formulation with poor toughenability). Both epoxies were modified with 15 wt% CTBN (carboxyl-terminated butadiene-acrylonitrile copolymer), that phase-separated in the course of polymerization.

Toughening mechanisms were analyzed by observing the damage zone around the surviving crack tip produced by the double-notch four-point-bend (DN-4PB) technique [4, 7–16]. Both transmission optical microscopy (TOM) and transmission electron microscopy (TEM) were used. The mechanical behavior of both unmodified epoxy matrices was analyzed in uniaxial compression. This is a useful test for studying yielding and strain softening since, because the stress is compressive, tensile fracture is suppressed and plastic yielding can be obtained for materials that under other conditions exhibit a brittle behavior.

## 2. Experimental

### 2.1. Materials

Two different epoxy matrices based on diglycidylether of bisphenol A (DGEBA, MY790, Ciba) were investigated. The first one was cured with piperidine (5 g per 100 g of DGEBA), during 16 h at 120 °C. The second one was cured with a stoichiometric amount of 4,4′-diamino-3,3′-dimethyldicyclohexylmethane (3DCM, Laromin C260, BASF), using the following thermal cycle: 1 h at 50 °C, 2 h at 100 °C and 2 h at 150 °C. Fig. 1 shows the chemical structures of the corresponding epoxy networks. The DGEBA-piperidine network (Fig. 1(a)) is generated by the chainwise anionic polymerization of epoxy groups. In spite of its high crosslink density, the high flexibility of polyether chains leads to a low-$T_g$ epoxy network. The DGEBA-3DCM network (Fig. 1(b)) is generated by the stepwise reaction of amine hydrogens with epoxy groups, leading to a (relatively) high-$T_g$ epoxy network.

A carboxyl-terminated butadiene-acrylonitrile copolymer (CTBN) was used as rubber modifier (Hycar 1300 × 9, Goodrich). The rubber-modified epoxies were prepared by first mixing the DGEBA with the appropriate rubber amount

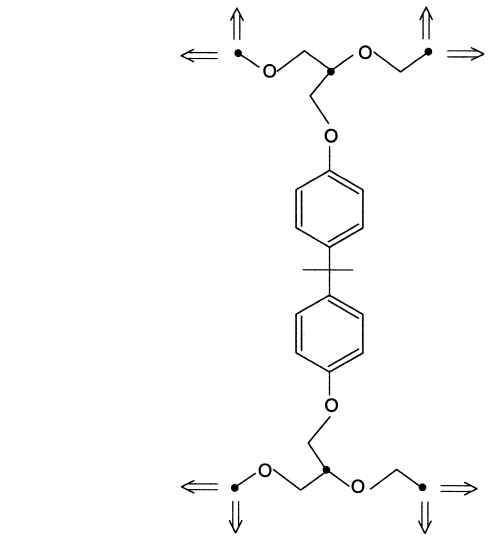


Fig. 1. Chemical structures of the epoxy networks generated by curing DGEBA with piperidine (a), and with 3DCM (b).

to give 15 wt% CTBN in the cured epoxy. Mixtures were degassed in a vacuum oven during 1 h at 80 °C. Then the curing agent was dissolved and the solution was poured into a preheated mold and cured in an oven with the selected thermal cycle.

Samples for subsequent mechanical characterization were machined from the molded materials (plates or cylinders), to reach final dimensions and improve surface finishing.

### 2.2. Electron microscopy

Fractured specimens were gold coated and then observed by scanning electron microscopy (SEM), using a Jeol JSM 35CF microscope. Samples to be studied by TEM were previously immersed in a 2 wt% $OsO_4$ aqueous solution during 2 days, to stain the C=C double bonds present in the rubber phase. Then a thin slice of about 80 nm was obtained by microtoming the specimen at room temperature and

observed by TEM (Jeol 100 CX microscope). The number-average diameter of rubber particles was determined using an image analyzer.

### 2.3. Thermal analysis

Differential scanning calorimetry (DSC) measurements were carried out with a Shimadzu DSC-50 device, by heating at a scanning rate of 10 °C/min under dry nitrogen. Glass transition temperatures ($T_g$) were determined at the onset of the transition.

### 2.4. Mechanical characterization

Mechanical tests were carried out at room temperature using an Instron 4467 universal testing machine. The flexural tangent elastic modulus, $E$, was determined following ASTM D790 standard at 2.8 mm/min. The yield behavior was studied under compression using cylindrical specimens, $L = 10$ mm and $d = 10$ mm, machined out from the cured materials. Care was taken to obtain smooth and parallel faces. No bubbles or internal flaws were revealed by visual inspection. Uniaxial compression tests were performed between flat dies at 1 mm/min. Barrelling was prevented by inserting poly(tetrafluoroethylene) sheets between the specimen faces and the dies. The compressive stress was calculated from the following equation

$$\sigma = P(1 - e)/A_0 \quad (1)$$

where $P$ is the load, $A_0$ is the initial cross-sectional area, and $e$ is the strain determined from the cross-head displacement, corrected for the machine softness. The true stress ($\sigma$) was plotted as a function of the true strain ($\varepsilon$). The intrinsic yield point ($\sigma_Y$) was taken as the point beyond which the deformation ceased to be recoverable on unloading. A set of specimens was strained to different $\varepsilon$ values, the load was removed and the strain relaxation was followed with time until a constant length was obtained (at about 15 days). By plotting the residual strain as a function of the maximum strain reached during the test, it was possible to determine the yield strain by extrapolation, and consequently, the yield stress from the stress–strain curve [17].

Fracture toughness was determined using linear elastic fracture mechanics. The critical stress intensity factor in plane strain, $K_{IC}$, was determined using a single-edge notched (SEN) type specimen (6.4 mm × 12.7 mm × 60 mm). Tests were performed according to ASTM D5045-93 standard. After making a notch at the center of the sample with a reciprocating saw, a sharp crack of length $a$ was initiated by tapping a fresh razor blade into the notch tip at room temperature [18]. The samples were tested in a 3-point bending mode at a cross-head speed of 10 mm/min. Reported results are the mean of at least eight samples. From load-line displacement plots and crack length, the stress intensity factor, $K$, was computed at maximum load from Eq. (2), where $f(a/W)$ is a dimensionless function of the ratio $a/W$, given by ASTM D5045 standard ($W$ is the height and $B$ is the thickness of the specimen)

$$K = \frac{P}{BW^{1/2}} f(a/W) \quad (2)$$

### 2.5. Analysis of the damage zone around the surviving crack tip

The double-notch four-point-bend (DN-4PB) technique was used to examine the damage zone around the surviving crack tip (Fig. 2). Two edge cracks of (almost) equal length were generated in the specimen (6.4 mm × 12.7 mm × 125 mm), that was then loaded using a four-point bending geometry, locating the two cracks in the tensile side within the minor span. Owing to stress intensification at the crack tips, a plastic zone is independently formed at each crack tip upon loading (the distance between cracks is larger than the size of the plastic zone). Because the cracks are not exactly identical, one of them becomes critical and propagates in an unstable manner, thus unloading the other crack which immediately becomes stationary.

TOM was employed to examine the damage zone around the surviving crack tip. Thin sections were obtained using the petrographic polishing technique [19]. First, a convenient block size was cut in a section normal to the fracture surface but parallel to the crack direction, and encapsulated in an epoxy formulation cured at room temperature. Samples were roughly ground, finely ground, roughly polished, and then finely polished. The polished surface was mounted onto a clean glass slide using an optically clear epoxy that was allowed to cure overnight at room temperature. Excess material was removed using a diamond saw and the sample was again ground and polished until the plane of interest was finally reached. The thickness of the final material ranged from 150 to 350 μm. Optical micrographs were taken using an Olympus SZH 10

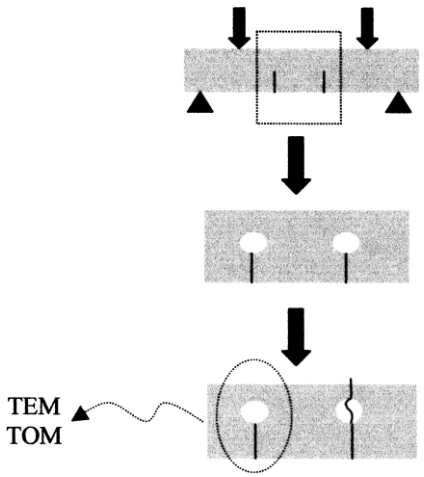


Fig. 2. Scheme of the double-notch four-point-bend (DN-4PB) technique.

transmission microscope, with an without crossed-polarizers.

A portion of the section cut for TOM analysis was carefully trimmed to an appropriate size, embedded in an epoxy resin and cured at room temperature. The block was further trimmed down to a size of about $0.5 \times 0.5$ mm$^2$, with the damage zone roughly placed at its center. It was then stained with $OsO_4$ and observed by TEM.

## 3. Results and discussion

### 3.1. Generated morphologies

For both rubber-modified epoxies, phase separation of a rubbery phase was produced in the course of polymerization. Fig. 3(a) and (b) shows TEM micrographs of the generated morphologies. The average size of rubber particles present in the DGEBA-3DCM system (0.17 μm) is lower than the corresponding average size for the DGEBA-piperidine system (0.77 μm). However, in the latter case a bimodal distribution seems to be present, with a large fraction of very small particles.

### 3.2. Thermal and mechanical characterization

Thermal and mechanical properties of pure and rubber-modified epoxies are shown in Table 1. The DGEBA-3DCM epoxy exhibits higher values of the glass transition temperature and the yield stress than the DGEBA-piperidine

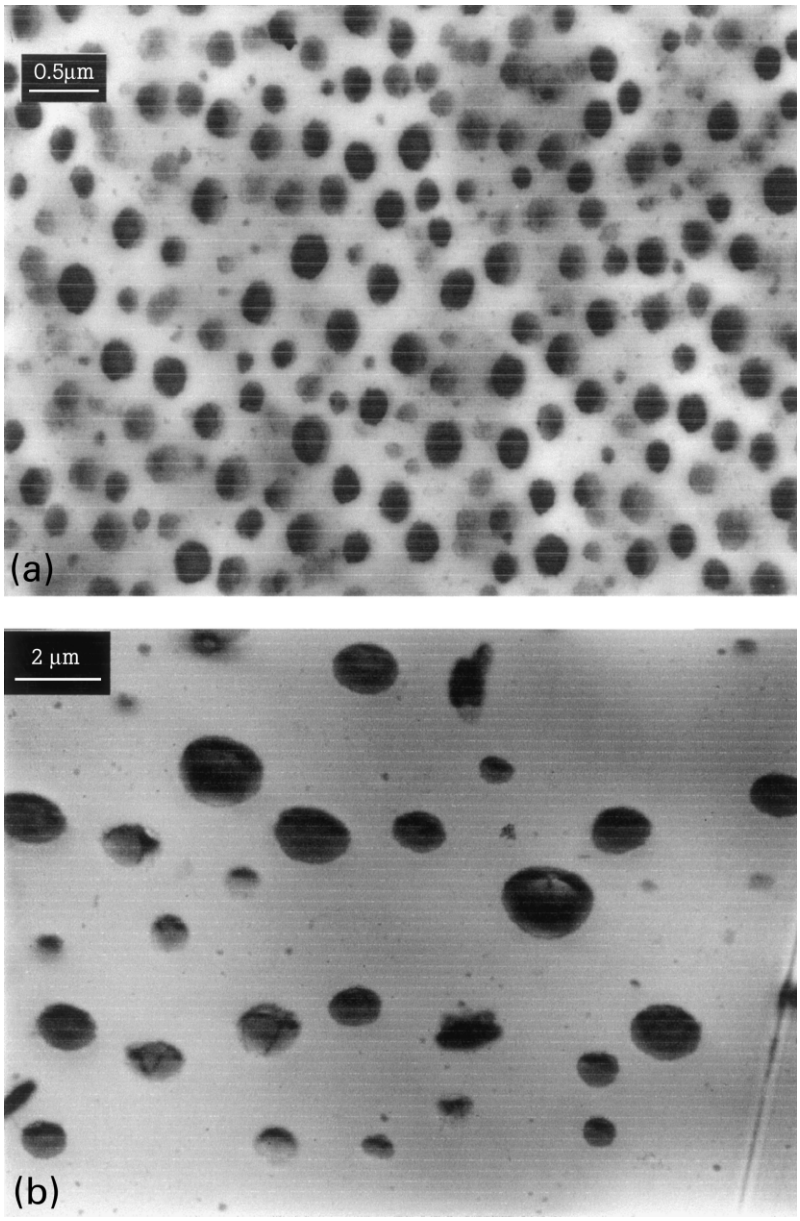


Fig. 3. TEM micrographs of rubber-modified epoxies: (a) DGEBA-3DCM, (b) DGEBA-piperidine.

Table 1
Thermal and mechanical properties of pure and rubber-modified epoxies

| Material | $T_g$ (°C) | $E$ (GPa) | $\sigma_Y$ (MPa) | $\varepsilon_Y$ (MPa) | $K_{IC}$ (MPa m$^{1/2}$) |
|---|---|---|---|---|---|
| DGEBA-3DCM | 152 | 2.69 | 109 | 0.12 | 0.57 ± 0.03 |
| DGEBA-3DCM (+15% CTBN) | 132 | 1.93 | 78 | 0.10 | 1.14 ± 0.07 |
| DGEBA-piperidine | 79 | 2.75 | 92 | 0.05 | 0.92 ± 0.12 |
| DGEBA-piperidine (+15% CTBN) | 77 | 1.73 | 63 | 0.06 | 1.97 ± 0.12 |

system. This is due to the flexibility of polyether chains present in the structure of the latter. It is interesting to note that the crosslink density is higher, and the molar mass between crosslinks lower, in the DGEBA-piperidine system than in the DGEBA-3DCM network. As $T_g$ depends both on crosslink density and chain flexibility [1], the yield strength should be better associated to the $T_g$ value rather than to the crosslink density (the incorrect association of toughenability with crosslink density is frequently found in the literature). The elastic modulus in the glassy state, that depends on the cohesive energy density and the intensity of sub-glass transitions [1], is almost the same for both epoxy networks.

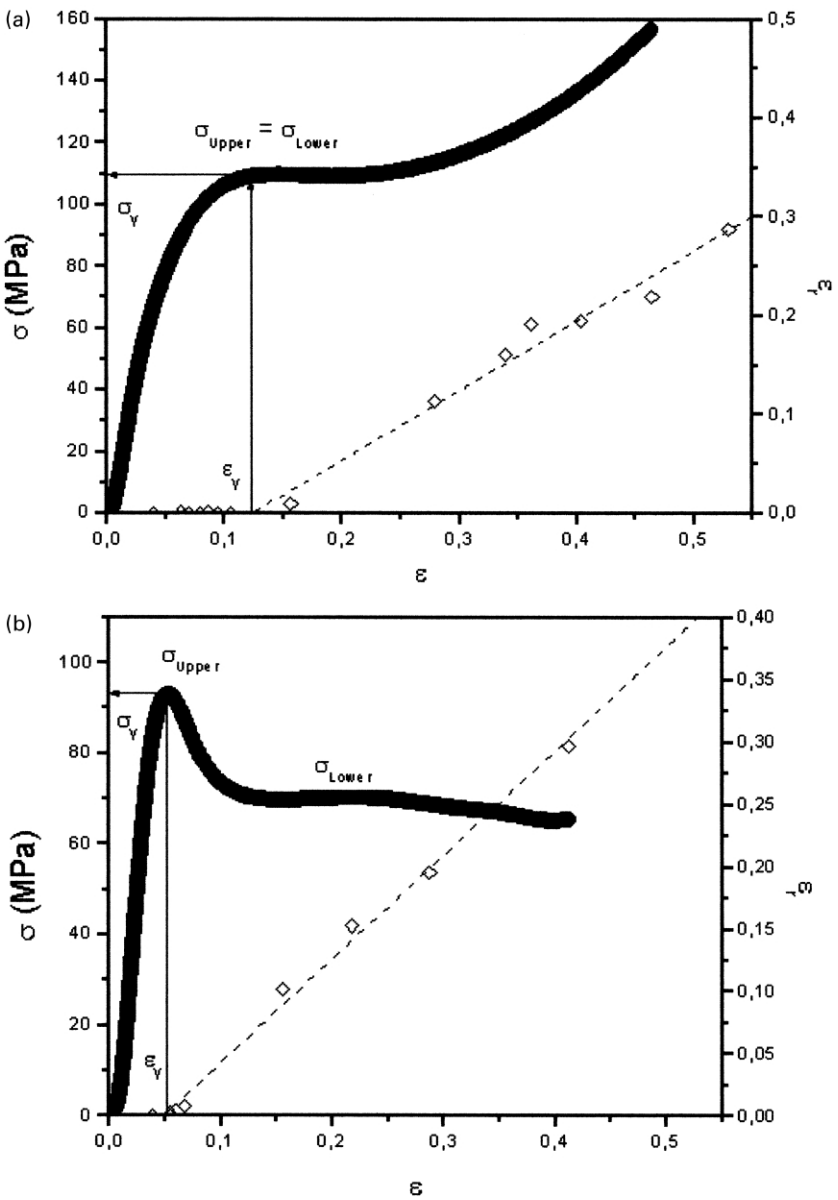


Fig. 4. True stress vs. true strain curves obtained in uniaxial compression tests of pure epoxies; (a) DGEBA-3DCM, (b) DGEBA-piperidine. The residual strain, plotted as a function of the initial strain enables the determination of the yield stress.

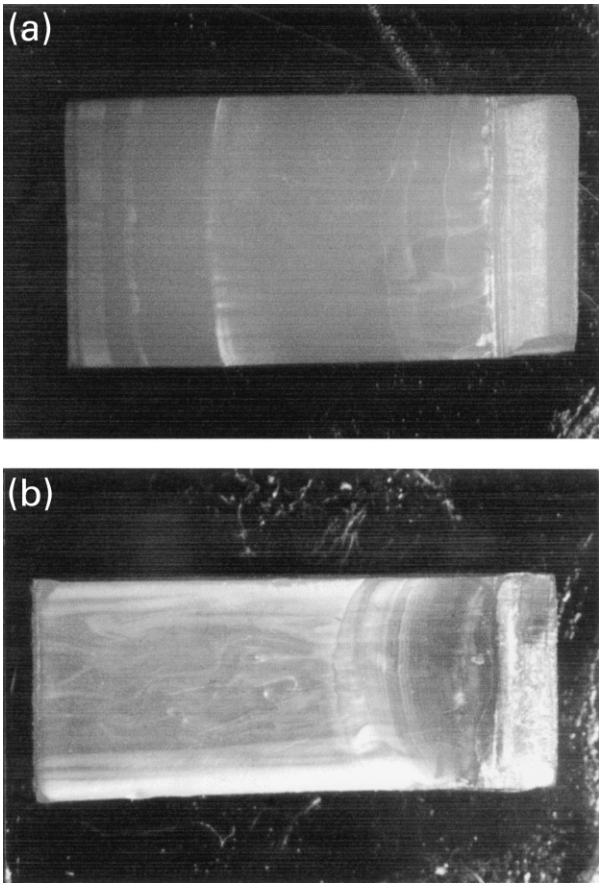


Fig. 5. Fracture surfaces: (a) rubber-modified DGEBA-3DCM, (b) rubber-modified DGEBA-piperidine.

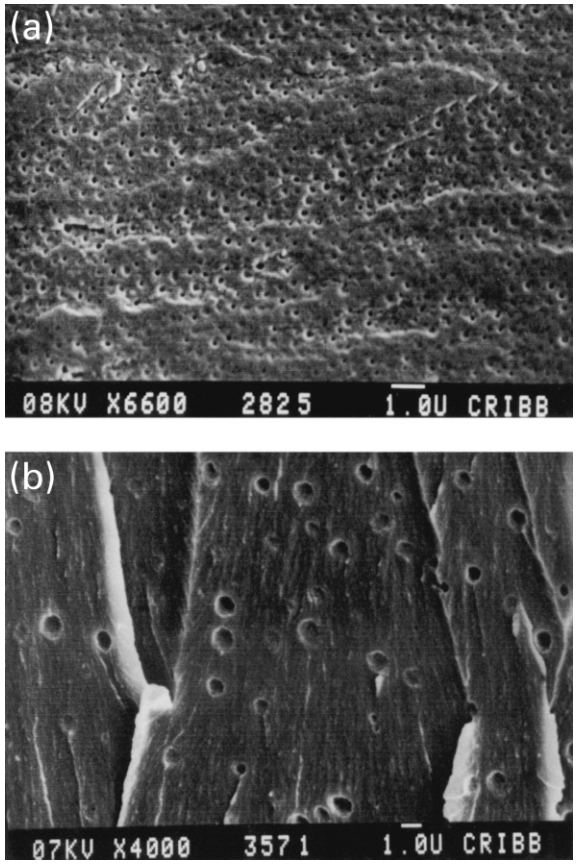


Fig. 6. SEM micrographs of the region close to the crack tip: (a) rubber-modified DGEBA-3DCM, (b) rubber-modified DGEBA-piperidine.

The response of pure epoxies in uniaxial compression tests is shown in Fig. 4. Residual strains, plotted as a function of initial strains, enable to locate the yield stress in the stress–strain curve. A significant difference in the behavior of the two epoxies is observed. While the DGEBA-piperidine epoxy undergoes significant strain softening after yielding and exhibits a plateau stress persisting to relatively high strains, the DGEBA-3DCM epoxy does not undergo strain softening and shows strain hardening at relatively small strains. This, again, reveals the influence of chemical structure on the large-deformation behavior. The oxygen atom present in polyether chains of DGEBA-piperidine, acts as a hinge in the network structure, enabling different conformations of neighboring groups. This facilitates chain orientation and extension to large strains at relatively low stresses (strain hardening in the epoxy-piperidine matrix is observed at large strains [20]).

Thermal and mechanical properties of the rubber-modified epoxies changed in the expected way. A decrease in the glass transition temperature is the result of a fraction of rubber remaining dissolved in the matrix at the end of the polymerization. The epoxy network formed in the presence of piperidine was very effective in producing an almost complete phase separation of the liquid rubber (the decrease in $T_g$ was not significant). For the DGEBA-3DCM epoxy, a considerable fraction of rubber remained dissolved in the matrix, leading to a decrease of 20 °C in the $T_g$ value.

The elastic modulus in the glassy state decreases with increasing the volume fraction of the soft rubber particles, following a rule of mixtures. The observed decrease was higher for the DGEBA-piperidine system, giving an indirect evidence of the fact that the volume fraction of dispersed rubber was higher for this material. This agrees with the conclusion arising from the analysis of $T_g$ values.

The two rubber-modified epoxies showed a significant decrease in the yield stress with respect to the values obtained for the neat epoxy matrices. This results from the stress concentration effect produced by the dispersed particles [6,21]. Besides, as $\sigma_Y$ depends on $(T_g - T)$ [22], for the DGEBA-3DCM system the decrease of $T_g$ should also contribute to the observed decrease in the yield stress.

### 3.3. Fracture tests

Experimental values of the critical stress intensity factors, $K_{IC}$, exhibited an inverse correlation with the yield stress values (Table 1). This is the same trend reported in the literature for unmodified epoxies, and explained by the crack tip blunting model [23,24]. Although the relative increase in $K_{IC}$ is similar for both epoxy formulations, the effect of the rubber addition must be taken from $\Delta K_{IC}$

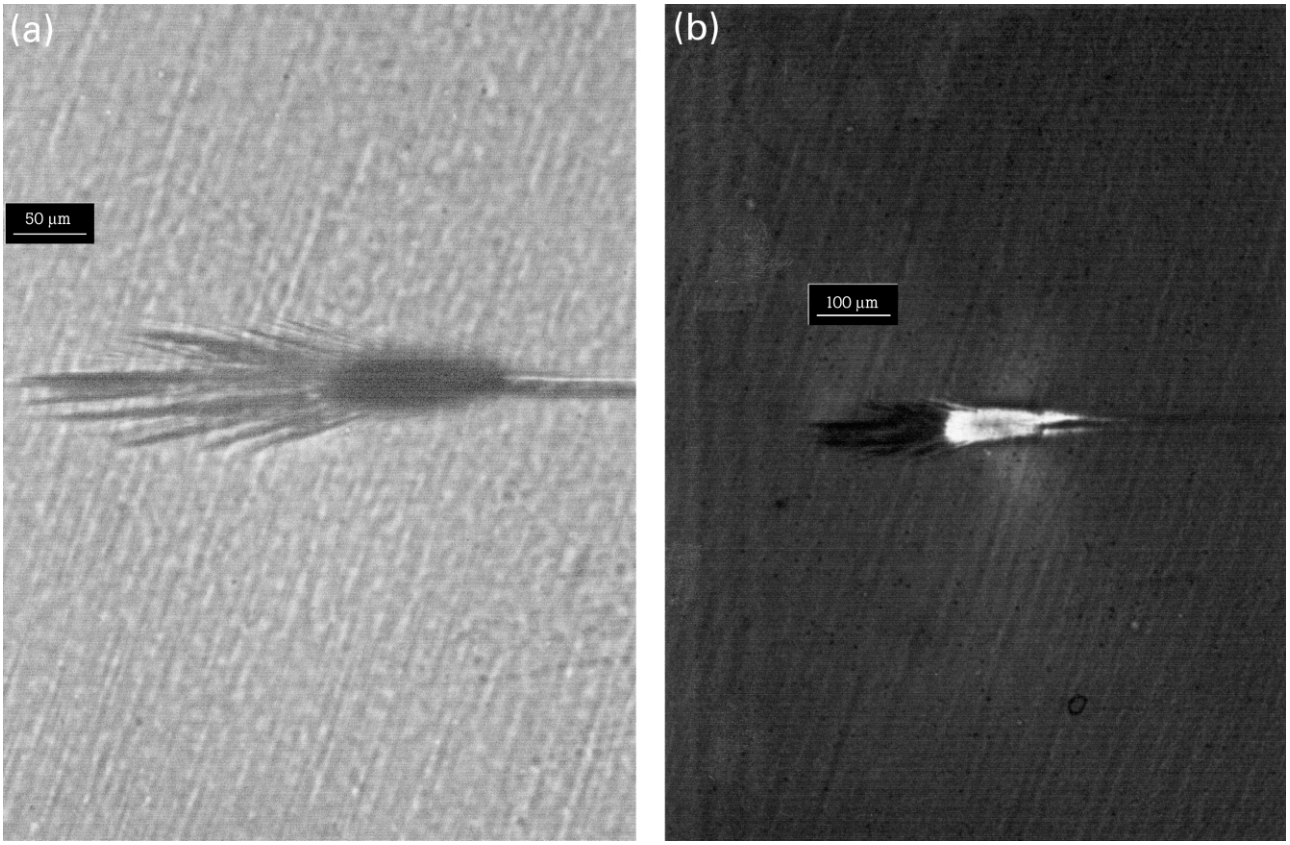


Fig. 7. TOM micrographs of the region around the surviving crack tip in the rubber-modified DGEBA-piperidine epoxy; (a) without crossed-polarizers, (b) with crossed-polarizers.

values. This analysis shows that the rubber is more effective for the epoxy-piperidine system than for the DGEBA-3DCM formulation. However, with evidence only from $K_{IC}$ values it is not possible to state if the observed increase in the fracture resistance is merely the result of crack tip blunting generated by the decrease in the yield stress. The occurrence of toughening mechanisms associated with the presence of rubber particles may be inferred from the analysis of fracture surfaces.

The examination of fracture surfaces (Fig. 5) revealed significant differences in the crack propagation modes. The rubber-modified DGEBA-3DCM epoxy showed a very smooth and mirror-like fracture surface with stick/slip propagation marks on it. This was consistent with crack-arrest followed by re-initiation, observed in load–displacement curves of fracture tests. Stick/slip propagation is caused by crack tip blunting due to localized plastic stretching [2]. On the contrary, the rubber-modified DGEBA-piperidine system exhibited a stable propagation in load–displacement curves and the presence of a stress-whitened region close to the initial crack tip. This region corresponds to the slow crack growth zone and its opacity may be associated to the presence of a large number of cavitated rubber particles.

However, SEM micrographs taken in the region close to the crack tip (Fig. 6), revealed the presence of cavitated rubber particles in both rubber-modified epoxies. Possibly, the stress-whitened zone was not observed in the rubber-modified DGEBA-3DCM epoxy due to the small size of cavitated particles. Therefore, this experimental evidence alone does not suffice to assess the efficiency of rubber addition on promoting additional toughening mechanisms in the two rubber-modified epoxies.

### *3.4. Analysis of the damage zone around the surviving crack tip*

Fig. 7 shows TOM micrographs of the region close to the surviving crack tip in the rubber-modified DGEBA-piperidine epoxy. Two regions are present. The first one that extends for about 100 μm right in front of the crack tip, appears dark without crossed-polarizers and becomes bright with crossed-polarizers. The second one is located ahead of the first zone and is composed of a large number of bands extending in different directions that are enclosed in a small angle with respect to the direction of crack propagation.

The first zone is clearly the result of the cavitation of rubber particles followed by void growth and induced shear yielding of the matrix. Cavitated particles produce the dark region without crossed-polarizers. But the region turns bright in the presence of crossed-polarizers, due to the partial orientation of

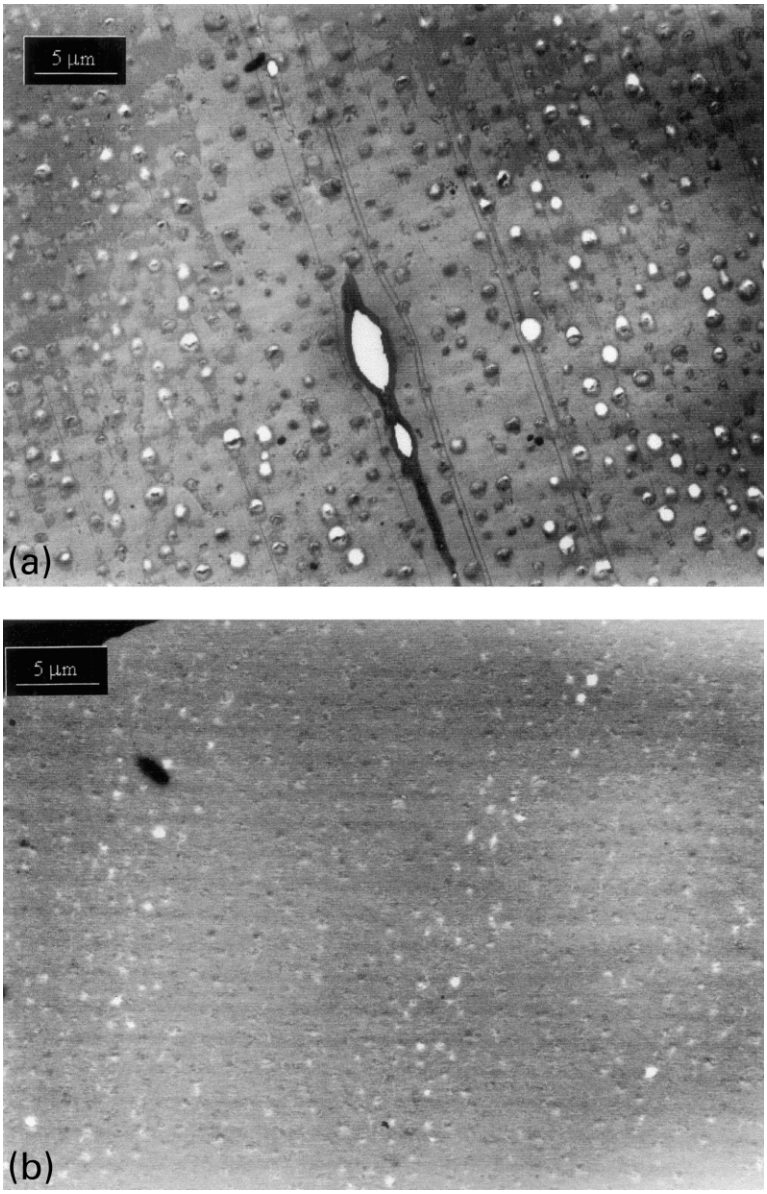


Fig. 8. TEM micrographs of the damage region around the surviving crack tip in the rubber-modified DGEBA-piperidine epoxy; (a) region in front of the crack tip (first zone), (b) region located ahead of the first zone (second zone).

elastic chains produced by massive shear yielding of the matrix that leads to an anisotropic material.

The second zone is assigned to the formation of dilatation bands that did not yet provoke massive shear yielding of the surrounding matrix. The angle between one of these bands and the principal tensile axis is expected to be less than 38° in uniaxial tension, depending upon its void content [6].

TEM micrographs of the same region are shown in Fig. 8. The first zone (Fig. 8(a)) shows the presence of a large fraction of cavitated rubber-particles located around the crack tip. Besides, crack propagation through cavitated rubber particles is observed (the presence of rubber is evidenced by the $OsO_4$ staining). The second zone (Fig. 8(b)) shows the presence of arrays of cavitated rubber particles, confirming the presence of dilatation bands.

Cavitation of rubber particles followed by void growth and induced shear yielding of the matrix is the accepted main toughening mechanism of rubber-modified epoxies [2]. But, as discussed by Bucknall [6], due to the presence of strain softening in the epoxy matrix yielding tends to become localized into dilatation bands which are planar zones of high shear strain. Elastically strained material around the edges of the bands becomes strain softened, allowing the band to extend in area. The overlapping of dilatation bands produces massive shear yielding of the matrix. Hardening eventually imposes a limit on the strain achieved. The sequence of events seems to be cavitation, growth of holes with the simultaneous formation of dilatation bands (second zone), and massive shear yielding by overlapping of dilatation bands (first zone). The

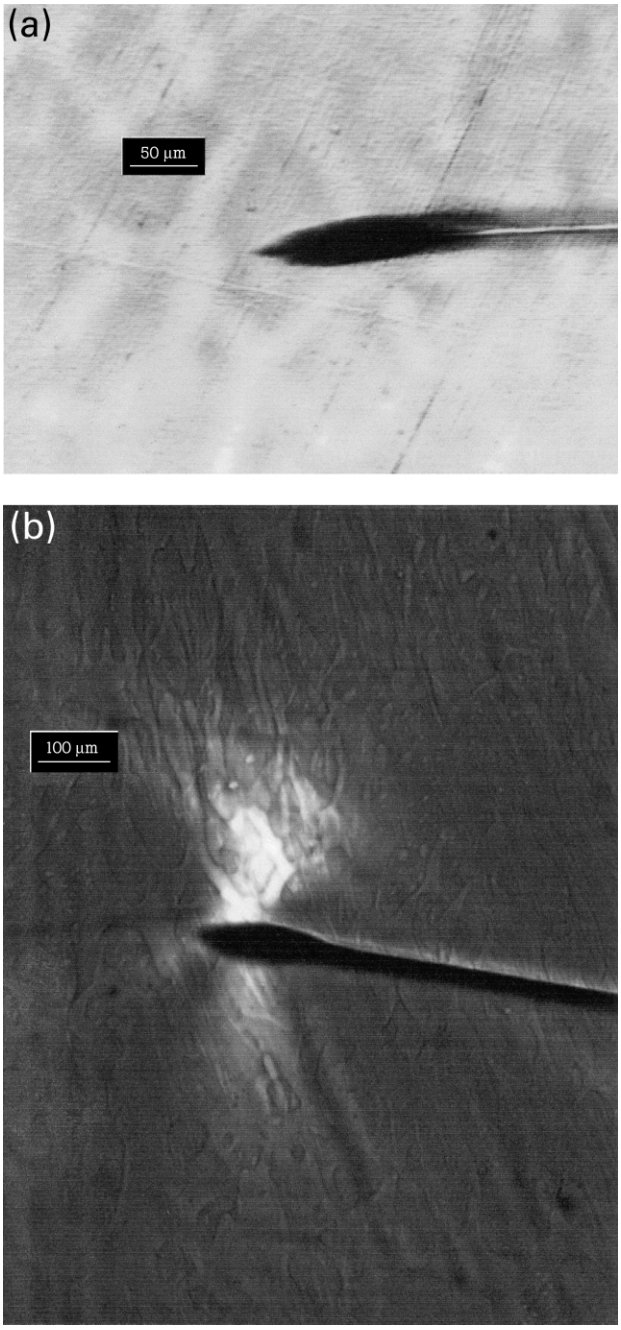


Fig. 9. TOM micrographs of the region around the surviving crack tip in the rubber-modified DGEBA-3DCM epoxy; (a) without crossed-polarizers, (b) with crossed-polarizers.

contributions of the epoxy matrix to generate this toughening mechanism are its low yield stress produced by rubber addition, and its ability to produce strain softening keeping a relatively low stress value in a large deformation range.

TOM micrographs of the region around the surviving crack tip in the rubber-modified DGEBA-3DCM epoxy are shown in Fig. 9. Only the region of cavitated particles is present around the crack tip. But this region appeared dark both with and without crossed-polarizers meaning that matrix shear yielding did not take place (the bright region observed using crossed-polarizers is ascribed to the presence of residual stresses generated during the encapsulation of the sample with the room-temperature cured epoxy). The presence of cavitated rubber particles was confirmed by the TEM micrograph taken in the region close to the crack tip (Fig. 10). Therefore, rubber modification of the DGEBA-3DCM matrix was only effective to decrease the yield stress promoting the increase in $K_{IC}$ through crack tip blunting. In spite of the fact that rubber cavitation did take place, growth of holes with simultaneous formation of dilatation bands was not observed. The contribution of rubber cavitation to the observed increase in $K_{IC}$, may be assumed to be very small. The poor toughenability of this epoxy may be associated to its inability to undergo large deformations at relatively low stress values (Fig. 4(a)). Without the possibility of provoking shear deformation in the matrix, cavities inside rubber particles are not stabilized and develop into a crack propagating through the ligament between neighboring particles. This provokes a fast crack propagation process and premature fracture of the sample.

## 4. Conclusions

The mere increase of $K_{IC}$ by rubber-modification should not be used, as is frequently found in the literature, as a criterion for assessing its efficiency on the toughening of an epoxy formulation. The stress concentration effect produced by dispersed particles and the decrease in the glass transition temperature produced by the fraction of rubber remaining dissolved in the matrix, lead to a decrease in $\sigma_Y$ and a corresponding increase in the critical stress intensity factor, $K_{IC}$, originated by crack tip blunting. The toughenability of an epoxy matrix should be defined by its ability to promote deformation mechanisms that can increase $K_{IC}$ beyond the value attained by the decrease in the yield stress. From the analysis of the damage zone around the surviving crack tip

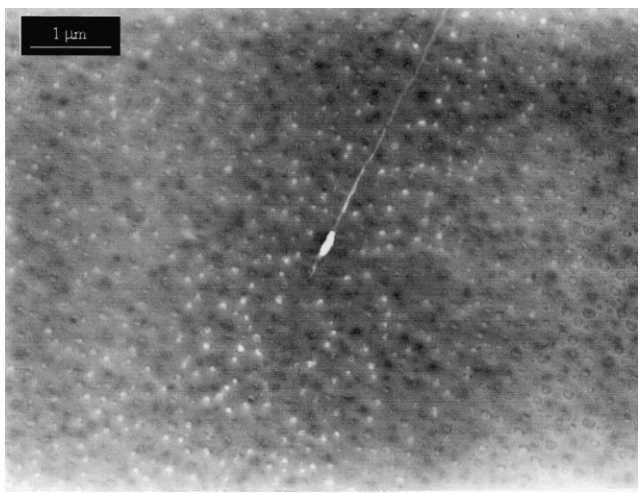


Fig. 10. TEM micrograph of the damage region around the surviving crack tip in the rubber-modified DGEBA-3DCM epoxy.

in two rubber-modified epoxy systems, and the behavior of the neat matrices in uniaxial compression tests, it was shown that the generation of significant toughening mechanisms may be related to the ability of the epoxy matrix to undergo strain softening followed by large deformations at relatively low stress values. This enables the formation of dilatation bands that extend in area, leading to massive shear yielding of the material located in the region close to the crack tip.

## Acknowledgements

The authors are grateful to Drs Carina Cano and María J. Yañez for carrying out the electronic microscopy experiments.

## References

[1] Pascault JP, Sautereau H, Verdu J, Williams RJJ. Thermosetting polymers. New York: Marcel Dekker; 2002.
[2] Yee AF, Du J, Thouless MD. In: Paul DR, Bucknall CB, editors. Polymer blends: performance, vol. 2. New York: Wiley; 2000. p. 225–67. Chapter 26.
[3] Pearson RA, Yee AF. J Mater Sci 1989;24:2571–80.
[4] Sue HJ. J Mater Sci 1992;27:3098–107.
[5] Lazzeri A, Bucknall CB. J Mater Sci 1993;28:6799–808.
[6] Bucknall CB. In: Paul DR, Bucknall CB, editors. Polymer blends: performance, vol. 2. New York: Wiley; 2000. p. 83–117. Chapter 22.
[7] Sue HJ, Yee AF. J Mater Sci 1989;24:1447–57.
[8] Parker DS, Sue HJ, Huang J, Yee AF. Polymer 1990;31:2267–78.
[9] Wu J, Mai YW. J Mater Sci 1993;28:6167–77.
[10] Pearson RA, Yee AF. J Mater Sci 1991;26:3828–44.
[11] Sue HJ, Garcia-Meitin EI, Orchard NA. J Polym Sci, B: Polym Phys 1993;31:595–608.
[12] Bagheri R, Pearson RA. Polymer 1996;37:4529–38.
[13] Cardwell BJ, Yee AF. J Mater Sci 1998;33:5473–84.
[14] Kim ST, Kim JK, Lim S, Choe CR, Hong SI. J Mater Sci 1998;33:2421–9.
[15] Lee J, Yee AF. Polymer 2000;41:8363–73.
[16] Hwang JW, Park SD, Cho K, Kim JK, Park CE, Oh TS. Polymer 2000;38:1835–43.
[17] Rose J, Duckett RA, Ward IM. J Mater Sci 1995;30:5328–34.
[18] Xiao K, Ye L, Kwok YS. J Mater Sci 1998;33:2831–6.
[19] Holick AS, Kambour RP, Fink DG, Hobbs SY. Microstruct Sci 1979;7:357–67.
[20] Kinloch AJ, Finch CA, Hashemi S. Polym Commun 1987;28:322–5.
[21] Gloagen JM, Steer P, Galliard P, Wrotecki C, Lefebvre JM. Polym Engng Sci 1993;33:748–53.
[22] Tcharkhtchi A, Trotignon JP, Verdu J. Macromol Symp 1999;147:221–34.
[23] Kinloch AJ, Williams JG. J Mater Sci 1980;15:987–96.
[24] Huang Y, Kinloch AJ. Polymer 1992;33:5338–40.